Applied Physics Letters

First harmonic measurements of the spin Seebeck effect

Cite as: Appl. Phys. Lett. **113**, 202403 (2018); https://doi.org/10.1063/1.5053120
Submitted: 21 August 2018 . Accepted: 23 October 2018 . Published Online: 15 November 2018

Yizhang Chen, Debangsu Roy, Egecan Cogulu, Houchen Chang, Mingzhong Wu, and Andrew D. Kent

View Online Export Citation CrossMark

ARTICLES YOU MAY BE INTERESTED IN

Anomalous Hall effect in thin films of the Weyl antiferromagnet Mn_3Sn
Applied Physics Letters **113**, 202402 (2018); https://doi.org/10.1063/1.5064697

Angle dependent magnetoresistance in heterostructures with antiferromagnetic and non-magnetic metals
Applied Physics Letters **113**, 202404 (2018); https://doi.org/10.1063/1.5049566

Conversion of spin current into charge current at room temperature: Inverse spin-Hall effect
Applied Physics Letters **88**, 182509 (2006); https://doi.org/10.1063/1.2199473

Lock-in Amplifiers up to 600 MHz
Watch

© 2018 Author(s).

First harmonic measurements of the spin Seebeck effect

Yizhang Chen,[1,a)] Debangsu Roy,[1,a)] Egecan Cogulu,[1] Houchen Chang,[2] Mingzhong Wu,[2] and Andrew D. Kent[1,b)]
[1]*Center for Quantum Phenomena, Department of Physics, New York University, New York, New York 10003, USA*
[2]*Department of Physics, Colorado State University, Fort Collins, Colorado 80523, USA*

(Received 21 August 2018; accepted 23 October 2018; published online 15 November 2018)

We present measurements of the spin Seebeck effect (SSE) by a technique that combines alternating currents (AC) and direct currents (DC). The method is applied to a ferrimagnetic insulator/heavy metal bilayer, $Y_3Fe_5O_{12}$ (YIG)/Pt. Typically, SSE measurements use an AC current to produce an alternating temperature gradient and measure the voltage generated by the inverse spin-Hall effect in the heavy metal at twice the AC frequency. Here, we show that when Joule heating is associated with AC and DC bias currents, the SSE response occurs at the frequency of the AC current drive and can be larger than the second harmonic SSE response. We compare the first and second harmonic responses and show that they are consistent with the SSE. The field dependence of the voltage response is used to distinguish between the damping-like and field-like torques. This method can be used to explore nonlinear thermoelectric effects and spin dynamics induced by temperature gradients. *Published by AIP Publishing*. https://doi.org/10.1063/1.5053120

A central theme in spintronics is the interconversion of charge and spin currents.[1] Recently, a focus has been on magnetic insulators where spin transport occurs through spin-wave propagation and spin currents can be generated by either spin injection[2] or thermal gradients.[3,4] These phenomena can be studied in simple bilayer films consisting of a ferrimagnetic (FIM) insulator, such as $Y_3Fe_5O_{12}$ (YIG), and a heavy metal (HM) with large spin-orbit coupling such as Pt. Spin to charge current conversion in such bilayers occurs by the inverse spin-Hall[5–7] and Rashba-Edelstein effects.[8,9]

Spin to charge conversion enables determination of the spin Seebeck effect (SSE).[10–13] A thermal gradient across the FIM film produces a spin current into a neighboring heavy metal film, resulting in a transverse charge current or a voltage across the heavy metal film in an open circuit situation. Recent studies have demonstrated significant torques associated with thermally generated spin currents in magnetic tunnel junctions.[14,15] The spin Nernst effect with an in-plane temperature gradient has also been shown to provide a means to generate spin currents.[16,17] Thermal gradients, thus, provide a convenient route to characterize the spin transport as well as a means to study the inverse effects, such as the spin torque on the FIM magnetization in response to spin currents associated with charge current flow in the HM. In fact, the SSE also enables detection of the FIM magnetization direction by relatively simple electrical measurements.

In this article, we present first harmonic measurements of the SSE by a technique that combines AC and DC currents in a YIG/Pt bilayer. The temperature gradient is created by Joule heating in a Pt strip and both the linear and nonlinear responses in the longitudinal and transverse voltages are determined as a function of the angle between the AC current and an in-plane external magnetic field. An analysis of the responses shows that the SSE accounts for the main component of the second harmonic voltage response, corroborating results in the literature.[18] However, when a DC current is present, several new features are observed. First, we detect field-induced switching of the YIG magnetization in both the first and second harmonic longitudinal voltage measurements. Second, both the first and second harmonic transverse voltages show a step when the magnetization reverses. Interestingly, the step height in the first harmonic response has a linear dependence on DC current density and cosine dependence on the in-plane field angle. Of particularly interest is that the presence of a DC current superposed on the AC current enables measurements of the SSE in the first harmonic response with an increase in signal amplitude relative to the second harmonic signal.

The samples we studied consist of a 20 nm thick epitaxial YIG film grown on a gadolinium gallium garnet ($Gd_3Ga_5O_{12}$) substrate by RF sputtering[19] and a 5 nm thick Pt film grown by DC sputtering in separate deposition systems. The YIG film is transferred in air and Ar^+ plasma cleaning is performed prior to the deposition of the Pt film. A Hall bar with a width of 4 μm and a length between the voltage contacts of 90 μm is fabricated using e-beam lithography and ion milling. The current flows in the x-direction and the voltage is measured both along the current direction (V_{xx}) and transverse to the current direction (V_{xy}) with separate electrical contacts [Fig. 1(a)]. Lock-in amplifiers are used to measure the first harmonic and second harmonic voltages with phases $\phi_1 = 0°$ and $\phi_2 = -90°$ and a time constant of 300 ms. The AC current frequency is 953 Hz, and its rms amplitude is indicated in the figures. All the angular dependent data are averaged 50 times to improve the signal-to-noise ratio. The measurements are conducted at room temperature.

Figures 1(b) and 1(c) show the second harmonic longitudinal $V_{xx}^{2\omega}$ and transverse $V_{xy}^{2\omega}$ voltage, respectively, as a function of the in-plane angle of a 400 mT magnetic field, a field sufficient to saturate the magnetization of the YIG layer. To

[a)]Y. Chen and D. Roy contributed equally to this work.
[b)]Electronic mail: andy.kent@nyu.edu

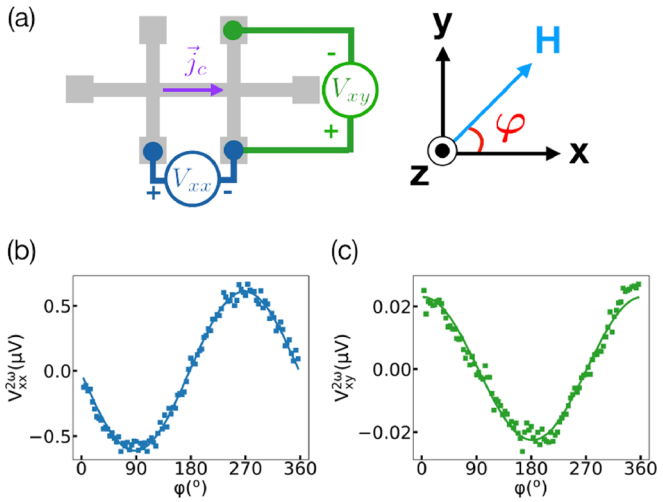

FIG. 1. (a) Measurement setup. $\vec{j}_c$ is the charge current density along the x direction. V_{xx} and V_{xy} are the voltages measured in the longitudinal and transverse directions, respectively, while φ is the angle between the applied field and the current. (b) Angular dependence of second harmonic longitudinal voltage $V_{xx}^{2\omega}$ at a fixed current density of $j_{ac} = 1.5 \times 10^{10}$ A/m^2 with an applied field of μ_0H = 400 mT. The curve is a fit to $V_{xx}^{2\omega}(0)\sin(\varphi)$. (c) Angular dependence of second harmonic transverse voltage $V_{xy}^{2\omega}$ at the same current density, $j_{ac} = 1.5 \times 10^{10}$ A/m^2. The curve is a fit to $V_{xy}^{2\omega}(0)\cos(\varphi)$.

confirm that the second harmonic signal is associated with the SSE, measurements were repeated as a function of the applied magnetic field magnitude.[20,21] These results are shown in the supplementary material. It is important to note that there are contributions to the second harmonic signal from the damping-like (DL) torque, field-like (FL) torque, and Oersted (Oe) fields. By characterizing the field dependence of the second harmonic response, these effects can be separated, particularly at small applied fields at which these torques and Oersted fields introduce additional structure in the angular dependence of the second harmonic signal. This is discussed in the supplementary material, where the relative contributions of SSE, DL, FL, and Oe field torques are determined.[20–22] We find that for an applied field of 400 mT, the second harmonic signal is dominated by the SSE.

Figures 2(a) and 2(b) show the field dependence of second harmonic $V_{xy}^{2\omega}$ [Fig. 2(a)] and first harmonic V_{xy}^{ω} [Fig. 2(b)] response with the field applied along the current direction ($\varphi = 0°$) at a fixed AC current density of 1.5×10^{10} A/m^2 as the DC component of the current density is varied, $j_{dc} = 0$, ± 2.5, $\pm 5.0 \times 10^{10}$ A/m^2. The SSE response is expected to change sign when the magnetization direction reverses, which is evident in Fig. 2(a) in the step change in $V_{xy}^{2\omega}$ near zero field at the coercivity of the YIG ($\mu_0 H_c \simeq 10$ mT).

We define the mean ΔV as the average voltage when the applied field $\mu_0 H > 25$ mT minus the average voltage when $\mu_0 H < -25$ mT, divided by 2

$$\Delta V \equiv (\overline{V_{\mu_0 H > 25\,mT}} - \overline{V_{\mu_0 H < -25\,mT}})/2.$$

In our field swept experiments, V_{xy}^{ω} and $V_{xy}^{2\omega}$ have abrupt steps in small fields, fields less than 25 mT, and then are nearly field independent. Thus, this average increases the signal-to-noise ratio. The error bars in Figs. 3 and 4 represent the standard deviation of this mean voltage.

The step in voltage in the second harmonic signal is nearly independent of the DC current. Interestingly, the first harmonic response depends systematically on the DC current. At zero DC current, there is virtually no response, only small signal variations near zero field. However, when the DC current density is non-zero, a clear voltage step is evident near zero field, with a change in voltage that depends on the DC current.

The magnitude of the first harmonic signal is about one order of magnitude larger than the second harmonic signal. In addition, the step in the first harmonic signal changes sign when the DC current is reversed. Figures 3(a) and 3(b) show how the steps in voltage depend on DC current. The step in the second harmonic signal $\Delta V_{xy}^{2\omega}$ [Fig. 3(a)] is slightly modified due to DC current, whereas there is a clear linear relation between the step in the first harmonic signal ΔV_{xy}^{ω} [Fig. 3(b)] and the DC current.

In order to understand this behavior, one needs to consider Joule heating by the AC and DC current through the Pt. This leads to a power dissipation given by

$$\begin{aligned} P &= \left[\sqrt{2} j_{ac}\cos(\omega t) + j_{dc}\right]^2 RA \\ &= \left[j_{ac}^2\cos(2\omega t) + 2\sqrt{2} j_{ac} j_{dc}\cos(\omega t) + j_{ac}^2 + j_{dc}^2\right] RA, \end{aligned} \tag{1}$$

where j_{ac} is the rms AC current density, R is the resistance of the Pt, and A its cross sectional area, the film thickness times the width of the current line. The temperature gradient ∇T_z is proportional to the power dissipation. It follows that the SSE voltage generated has the following form:

$$V_{ISHE} \propto j_{ac}^2\cos(2\omega t) + 2\sqrt{2} j_{ac} j_{dc}\cos(\omega t) + j_{ac}^2 + j_{dc}^2. \tag{2}$$

There is, thus, an SSE response at two times the oscillation frequency of the current, the second harmonic, 2ω, as expected, as well as a signal at frequency, ω, the first harmonic. Thus, the combination of AC and DC currents

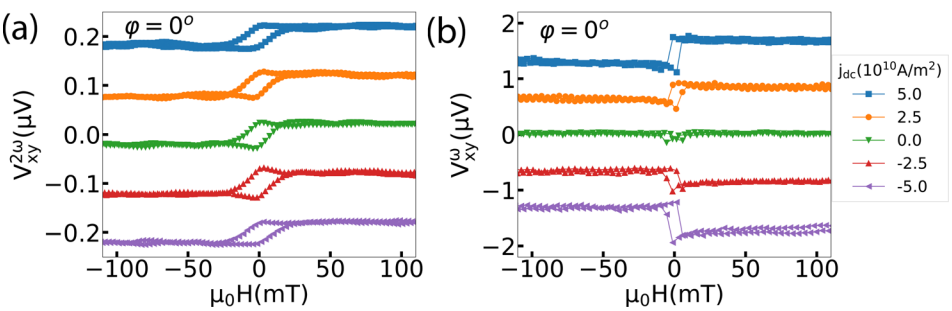

FIG. 2. Field dependent measurements of the second and first harmonic transverse voltages with fixed AC current $j_{ac} = 1.5 \times 10^{10}$ A/m^2 and varying DC currents. The curves are shifted vertically by a constant interval for clarity. (a) Field dependence of $V_{xy}^{2\omega}$ at $\varphi = 0°$ and $j_{dc} = 0$, ± 2.5, $\pm 5.0 \times 10^{10}$ A/m^2. (b) Field dependence of V_{xy}^{ω} with $\varphi = 0°$ and $j_{dc} = 0$, ± 2.5, $\pm 5.0 \times 10^{10}$ A/m^2.

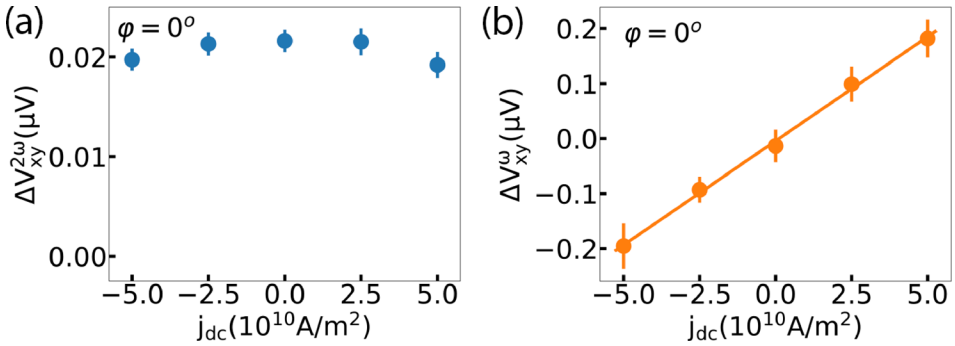

FIG. 3. Dependence of the second and first harmonic transverse voltage amplitudes on the DC current density with j_{ac} fixed at 1.5×10^{10} A/m^2. (a) Second harmonic transverse voltage versus DC current. (b) First harmonic transverse voltage versus DC current.

provides a technique to measure the SSE voltage as a first harmonic response. The relative magnitude of the first and the second harmonic signals is given by $V_{xy}^{\omega}/V_{xy}^{2\omega} = 2\sqrt{2}j_{dc}/j_{ac}$. The first harmonic response is, thus, about 2.8 times larger than the second harmonic response when the AC and DC currents are the same. The linear relation between ΔV_{xy}^{ω} and j_{dc} in Fig. 3(b) confirms this model.

Further, we experimentally verify the symmetry and magnitude of the SSE first harmonic response in comparison to the conventional second harmonic signal. We have performed field dependent measurements of the first harmonic transverse voltage by sweeping the external magnetic field between −400 mT and +400 mT at different in-plane angles φ from 0° to 360° at fixed $j_{ac} = 1.5 \times 10^{10}$ A/m^2 and $j_{dc} = \pm 5.0 \times 10^{10}$ A/m^2. Using these results, we have determined ΔV_{xy}^{ω} using the procedure mentioned in the preceding section and plot its variation with φ (Fig. 4). The SSE voltage is proportional to the projection of the magnetization on the axis perpendicular to the voltage probes. The temperature gradient is along the z-axis, whereas the spin polarization is along the YIG magnetization direction. Therefore, the angular dependence of the first harmonic and second harmonic transverse response is $V_{xy}^{\omega} \propto 2\sqrt{2}j_{ac}j_{dc}\cos(\varphi)$, $V_{xy}^{2\omega} \propto j_{ac}^2\cos(\varphi)$, as seen experimentally. Measurements of ΔV_{xy}^{ω} can be fitted well with $\Delta V_{xy}^{\omega}(0)\cos\varphi$, denoted by the solid line in Fig. 4. The second harmonic transverse voltage was measured with varying φ at a fixed field of +400 mT and a fixed $j_{ac} = 1.5 \times 10^{10}$ A/m^2 [Fig. 1(c)]. Equation (2) predicts that for $j_{ac} = 1.5 \times 10^{10}$ A/m^2 and $j_{dc} = \pm 5.0 \times 10^{10}$ A/m^2, the relative magnitudes of the first and second harmonic signals should be 9.4. We have extracted the maximum $\Delta V_{xy}^{\omega}(0) = 0.187 \pm 0.053\ \mu$V and $\Delta V_{xy}^{2\omega}(0) = 0.0227 \pm 0.0007\ \mu$V by fitting the data in Figs. 4 and 1(d), respectively. The experimentally obtained ratio of the first and second harmonic signals is 8.2 ± 2.7. The experimentally obtained ratio is, thus, consistent with our simple AC and DC current heating model. The data in Fig. 4 clearly indicate that the first harmonic response has a much higher signal-to-noise ratio than that of the second harmonic voltage [Fig. 1(c)].

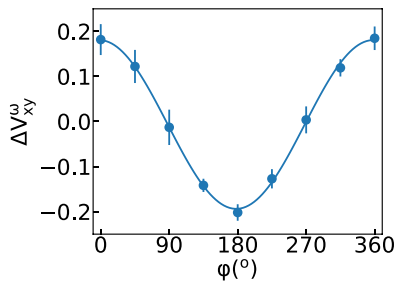

FIG. 4. Angular dependence of ΔV_{xy}^{ω} measured with an AC current of 1.5×10^{10} A/m^2 and a DC current of 5.0×10^{10} A/m^2. The curve is a fit to the data of the form $\Delta V_{xy}^{\omega}(0)\cos(\varphi)$.

In summary, we have determined the SSE-produced linear and nonlinear voltage responses in a YIG/Pt bilayer system. The second harmonic longitudinal voltage has a sine relation with respect to the in-plane field angle φ when the YIG is saturated. Angular dependence measurement of the longitudinal and transverse voltages as a function of the applied field magnitude enabled estimation of the contributions from SSE, DL, FL, and Oe field torques. It was found that the SSE dominates over the other contributions when the applied field is sufficient to saturate the YIG layer. In addition, by applying an AC current with DC bias, we determined that SSE can be measured by a first harmonic lock-in technique and can be more sensitive and have higher signal to noise than the conventional second harmonic method. This technique can be used to characterize the SSE in ferromagnetic (or ferrimagnetic) and non-magnetic bilayer systems as well as to study nonlinear thermoelectric effects and spin dynamics induced by temperature gradients.

See supplementary material section for measurements of the second harmonic longitudinal and transverse voltage response as a function of the applied field angle and magnitude. These data are analyzed to determine the relative contributions of the spin Seebeck effect, damping like, field-like, and Oersted field torque and how these contributions vary with the applied field.

The instrumentation used in this research was supported in part by the Gordon and Betty Moore Foundations EPiQS Initiative through Grant No. GBMF4838 and in part by the National Science Foundation under Award No. NSF-DMR-1531664. This work was supported partially by the MRSEC Program of the National Science Foundation under Award No. DMR-1420073. A.D.K. received support from the National Science Foundation under Grant No. DMR-1610416. At CSU, film growth was supported by the U.S. National Science Foundation (EFMA-1641989), and film characterization was supported by the U.S. Department of Energy, Office of Science, Basic Energy Sciences (DE-SC0018994).

[1]A. Brataas, A. D. Kent, and H. Ohno, Nat. Mater. **11**, 372 (2012).
[2]L. Cornelissen, J. Liu, B. van Wees, and R. Duine, Phys. Rev. Lett. **120**, 097702 (2018).

[3]K. Uchida, S. Takahashi, K. Harii, J. Ieda, W. Koshibae, K. Ando, S. Maekawa, and E. Saitoh, Nature **455**, 778 (2008).
[4]A. D. Avery, M. R. Pufall, and B. L. Zink, Phys. Rev. Lett. **109**, 196602 (2012).
[5]M. I. Dyakonov and V. I. Perel, Phys. Lett. A **35**, 459 (1971).
[6]J. E. Hirsch, Phys. Rev. Lett. **83**, 1834 (1999).
[7]S. Zhang, Phys. Rev. Lett. **85**, 393 (2000).
[8]J.-C. Rojas-Sanchez, L. Villa, G. Desfonds, S. Gambarelli, J. P. Attane, J. M. De Teresa, C. Magen, and A. Fert, Nat. Commun. **4**, 2944 (2013).
[9]K. Shen, G. Vignale, and R. Raimondi, Phys. Rev. Lett. **112**, 096601 (2014).
[10]K. Uchida, H. Adachi, T. Ota, H. Nakayama, S. Maekawa, and E. Saitoh, Appl. Phys. Lett. **97**, 172505 (2010).
[11]M. Schreier, N. Roschewsky, E. Dobler, S. Meyer, H. Huebl, R. Gross, T. Sebastian, and B. Goennenwein, Appl. Phys. Lett. **103**, 242404 (2013).
[12]D. Qu, S. Y. Huang, J. Hu, R. Wu, and C. L. Chien, Phys. Rev. Lett. **110**, 067206 (2013).
[13]T. Kikkawa, K. Uchida, Y. Shiomi, Z. Qiu, D. Hou, D. Tian, H. Nakayama, X.-F. Jin, and E. Saitoh, Phys. Rev. Lett. **110**, 067207 (2013).
[14]A. Pushp, T. Phung, C. Rettner, B. P. Hughes, S.-H. Yang, and S. S. P. Parkin, Proc. Natl. Acad. Sci. U. S. A. **112**, 6585 (2015).
[15]A. Bose, A. K. Shukla, K. Konishi, S. Jain, N. Asam, S. Bhuktare, H. Singh, D. D. Lam, Y. Fujii, S. Miwa, Y. Suzuki, and A. A. Tulapurkar, Appl. Phys. Lett. **109**, 032406 (2016).
[16]S. Meyer, Y.-T. Chen, S. Wimmer, M. Althammer, T. Wimmer, R. Schlitz, S. Gepraegs, H. Huebl, D. Koedderitzsch, H. Ebert, G. E. W. Bauer, R. Gross, and S. T. B. Goennenwein, Nat. Mater. **16**, 977 (2017).
[17]A. Bose, S. Bhuktare, H. Singh, S. Dutta, V. G. Achanta, and A. A. Tulapurkar, Appl. Phys. Lett. **112**, 162401 (2018).
[18]C. O. Avci, K. Garello, M. Gabureac, A. Ghosh, A. Fuhrer, S. F. Alvarado, and P. Gambardella, Phys. Rev. B **90**, 224427 (2014).
[19]H. Chang, P. Li, W. Zhang, T. Liu, A. Hoffmann, L. Deng, and M. Wu, IEEE Magn. Lett. **5**, 6700104 (2014).
[20]N. Vlietstra, J. Shan, B. J. van Wees, M. Isasa, F. Casanova, and J. Ben Youssef, Phys. Rev. B **90**, 174436 (2014).
[21]M. Hayashi, J. Kim, M. Yamanouchi, and H. Ohno, Phys. Rev. B **89**, 144425 (2014).
[22]C. O. Avci, K. Garello, J. Mendil, A. Ghosh, N. Blasakis, M. Gabureac, M. Trassin, M. Fiebig, and P. Gambardella, Appl. Phys. Lett. **107**, 192405 (2015).